

MICROSTRUCTURAL EVOLUTION AND GROWTH KINETICS OF INTERFACIAL COMPOUNDS IN TiAl/Ti₃SiC₂ DIFFUSION BONDING JOINTS

Guo-qing Chen¹, Qi Wang², Xue-song Fu³

¹School of Materials Science and Engineering, Dalian University of Technology, Dalian 116085, P. R. China, E-mail: gqchen@dlut.edu.cn

²School of Materials Science and Engineering, Dalian University of Technology, Dalian 116085, P. R. China, E-mail: 1018581889@qq.com

³School of Materials Science and Engineering, Dalian University of Technology, Dalian 116085, P. R. China, E-mail: xsfu@dlut.edu.cn

Keywords: Ti₃SiC₂, TiAl, Diffusion Bonding, Microstructural Evolution, Growth Kinetics.

ABSTRACT

TiAl intermetallic was direct diffusion bonded to Ti₃SiC₂ at 900°C, 950°C, and 1000°C with a holding time ranging from 0.25 h to 64 h. The interfacial microstructural evolution, the growth kinetics and the mechanical properties of the bonded TiAl/Ti₃SiC₂ joints were investigated in detail. The build-up of interfacial compounds in the TiAl/Ti₃SiC₂ joints changes from $\gamma+\alpha_2/\gamma/\text{Ti}_5\text{Si}_3/\text{Ti}_3\text{SiC}_2$, to $\gamma+\alpha_2/\gamma/\text{TiAl}_2/\text{Ti}_5\text{Si}_3/\text{Ti}_3\text{SiC}_2$, to $\gamma+\alpha_2/\gamma/\text{TiAl}_2/\text{Ti}_5\text{Si}_4/\text{Ti}_5\text{Si}_3/\text{Ti}_3\text{SiC}_2$, and to $\gamma+\alpha_2/\gamma/\text{TiAl}_2/\text{TiAl}_3+\text{Ti}_5\text{Si}_3/\text{Ti}_5\text{Si}_4/\text{Ti}_5\text{Si}_3/\text{Ti}_3\text{SiC}_2$ as the holding time or bonding temperature is increased. The de-intercalation Si atoms from the Ti₃SiC₂ diffusing into the TiAl base alloy and reacting with the Ti was found to be responsible for the formation of reaction layers in the interface. The thicknesses of the interfacial reaction layers grow following the parabolic kinetic law, indicated their growth was controlled by the bulk diffusion. The bonding activation energy was 213 kJ/mol. The highest shear strength of the joints was about 53 MPa bonded at 900°C for 9 h with a $\gamma+\alpha_2/\gamma/\text{TiAl}_2/\text{Ti}_5\text{Si}_4/\text{Ti}_5\text{Si}_3/\text{Ti}_3\text{SiC}_2$ interfacial microstructure with a total thickness of 6 μm .

1 INTRODUCTION

TiAl-based alloys are one of the most promising innovative high-temperature structural materials, due to their attractive “strong and light” properties, involving low density, high strength, excellent oxidation and creep resistance at elevated temperatures [1-3]. TiAl-based alloys are successfully used in aerospace and automotive [4, 5]. Dissimilar joining between Ti₃SiC₂ ceramic and TiAl intermetallic can blend their attractive property for the manufacturing of hybrid materials systems in harsh environments and enlarge their applications, particularly in the fast neutron reactor cladding materials and high temperature structure materials.

It is difficult to join ceramics with intermetallics when using conventional fusion welding techniques [6, 7]. Diffusion bonding is a feasible technology to bond the Mn+1AX_n ceramics to metals or intermetallics [8-10]. Basu and Kothalkar et al. [8, 11] investigated the interfaces between the diffusion bonded Ti₃SiC₂ and NiTi, and found that diffusion of Si from Ti₃SiC₂, and Ni from NiTi into reaction zone was responsible for the formation of reaction layers in the interface. Gao and Miyamoto [9] demonstrated that the total diffusion path of the Ti₃SiC₂ and TC4 diffusion bonded joining is Ti₃SiC₂/Ti₅Si₃Cx/Ti₅Si₃Cx+TiCx/TiCx/Ti. Liu and Cao et al. [12] studied the diffusion bonding of the TiAl intermetallic and the Ti₃SiC₂ ceramics, and found the interfacial microstructures of joints consist of TiAl/Ti₃Al₅/TiAl₂+Ti₅Si₃/Ti₅Si₃/Ti₃SiC₂ and remain unchanged between 1050°C to 1150°C. Although the phase constituent and the microstructures of the diffusion bonding TiAl/Ti₃SiC₂ joints under some conditions were investigated, the evolution of the microstructures, the atom diffusion behaviors, and the growth kinetics remain unknown. Since the interfacial microstructure has a great effect on bonding strength, a fundamental understanding of the microstructural evolution and growth kinetics of joints is desired for development of improved

processes. Recently, the Ti₃SiC₂ is considered a reinforcing phase or a protective coating for high-temperature structure materials to bend their good properties [13-18]. The challenge in fabricating these composites and coatings lies in controlling the interfacial microstructures. Systematic investigations of the underlying phenomena for the interfacial compounds formation and growth are of great interest to derive guidelines for the knowledge-based optimization of dissimilar joining and coating technology.

In this study, the evolution of the interfacial microstructures, the elemental diffusion behaviors, and the growth kinetics of the diffusion bonded TiAl/Ti₃SiC₂ joints were investigated in detail.

2 EXPERIMENTAL PROCEDURE

The Ti₃SiC₂ ceramic applied in this study was synthesized at 1465°C under 30 MPa for 2 h from 2TiC/1.05Ti/1.2Si (≥99.7%, Aladdin) powders via a hot-pressing route. The density of the Ti₃SiC₂ ceramic bulk was 4.43g/cm³. The purity was 98% according the X-ray diffraction pattern using the formulas in Ref. [19]. The TiAl base alloy with a nominal composition of Ti-44Al-4Nb-0.1B was prepared via powder metallurgy using pure element powders (≥99.7%, Aladdin) at 1300°C under 30 MPa for 3 h, followed by heat treatment at 1450°C for 2 h for a homogeneous composition. The microstructure of TiAl base alloy primarily consisted of γ/α_2 colonies.

The TiAl and Ti₃SiC₂ specimens (10.5 mm × 10.5 mm × 2 mm and 10 mm × 10 mm × 2 mm) were cut from the as-synthesized bulk (ϕ 60mm×27mm) by electrical-discharge machining. Prior to joining, the bonding surfaces of the TiAl and Ti₃SiC₂ samples were ground and polished to an optical finish, ultrasonically cleaned in ethanol, and dried by cold wind. The diffusion bonding was conducted in a hot-pressing furnace. Prior to heating, the furnace was pumped to 0.2 Pa and then filled into high purity Argon to 20 kPa to prevent oxidation. The heating and cooling rates were 10°C/min. The bond processes were conducted at 900°C, 950°C, and 1000°C with a holding time range between 0.25 h to 64 h under the same pressure of 50 MPa.

After the bonding process, the cross-sections of the bonded TiAl/Ti₃SiC₂ couples were cut with a diamond wire saw, then grinded and polished. The polished surface was etched using the wiping method by a solution consisting of 12% HF, 20% HNO₃, and 68% H₂O (volume percent). The interfacial microstructures of the obtained joints were characterized with scanning electron microscopy (SEM, Zeiss Supra 55). An electron micro probe analysis (EPMA, JEOL JXA-8530F Plus) was used for quantitative analysis of the various phases in the joints via spot analysis. Electron backscattered diffraction (EBSD) coupled with energy dispersive spectroscopy (EDS) mapping analysis was used to determine the reaction phases in the interface. An additional vibratory polishing step with 0.02 μ m colloidal silica solution by a vibratory polisher (Buehler VibroMet™ 2) was needed for the EBSD characterization. The shear strength tests were performed in a universal testing machine (DNS 100) under a cross-head drop speed of 0.5 mm/min at room temperature. At least 3 samples were examined to ensure the accuracy of the results.

3 RESULTS AND DISCUSSION

3.1 Microstructural evolution of the TiAl/Ti₃SiC₂ diffusion bonded interface

The back-scattered electron (BSE) images in Fig. 1 show typical interfacial microstructures of the samples bonded at 900°C/15 min, 950°C/1 h, and 1000°C/64 h. The morphology and the build-up of reaction layers changed by varying the duration and the bonding temperature. In order to identify the reaction phases, the elements quantitative analyses of each point in Fig. 1 were performed and the results are listed in Table 1. Some phases could not be confirmed from the element quantitative analyses. The electron backscatter diffraction (EBSD) observations were implemented on the interfaces. The color-coded phase maps and the elemental distribution maps are given in Fig. 2.

As shown Fig. 1(a), there are two new layers, a light grey phase adjacent TiAl substrate and a bright phase adjacent the Ti₃SiC₂, at the joint bonded at 900°C/15 min. The elements quantitative analysis results of points 2 and 3 in Table 1 shows that the light grey phase and the bright phase were the γ -TiAl and Ti₅Si₃ (more accurately Ti₅Si₃C_x), which were confirmed from the EBSD results in

Fig. 2(a). A new grey phase was present between the γ -TiAl layer and the Ti5Si3 layer in the interface bonding at 950°C/1 h shown in Fig. 1(b). This was TiAl2, as demonstrated from the results of the elements quantitative analysis of point 5 in Table 1 and the color-coded phase map in Fig. 2(b). When bonded at 950°C for 64h, a dual phase layer appeared between the TiAl2 phase and the bright region in Fig. 1(c). The black phase in the dual phase layer was TiAl3 (more accurately Ti(Al, Si)3) and the bright phase in the dual layer was Ti5Si3, according to the results from the EBSD and the elements quantitative analysis. There was a clear dividing line (white dashed-line) on the elements distribution images of the Si in Fig. 2(b). The bright region in Fig. 1(c) was not a single phase. The phase adjacent to the dual phase layer and the phase adjacent to the Ti3SiC2 substrate were recognized as Ti5Si4 and Ti5Si3 from the color-code phase images in Fig. 2(b). While the formation of Ti5Si4 was not previously observed in the TiAl/Ti3SiC2 diffusion couples [12]. This could be because the Ti5Si3 and Ti5Si4 were difficult to distinguish in the BSE images and were erroneously recognized as one phase. There was a straight line (yellow dashed-line) between the phase marked as Point 9 and the phase mark as Point 10 in Fig. 1(c). The phase on both sides of the straight line were the Ti5Si3 phase, as determined from the EBSD results. The different brightness of the Ti5Si3 at each sides of the straight line in Fig. 1(c) was due to the different Nb concentrations from the elements quantitative analysis results of Points 9 and 10 in Table 1. A similar result was found by comparing the element distribution maps of Nb and Si in Fig. 2(b). This could be because the bonding temperature was not adequate for the diffusion of the hard-diffusing Nb atoms in Ti5Si3, which remained at the initial place. So the straight line in Fig. 1(c) was a Kirkendall plane, which was confirmed from the bond contrast (BC) images in Fig. 2 because of their different microstructures (grain size and shape) [20, 21].

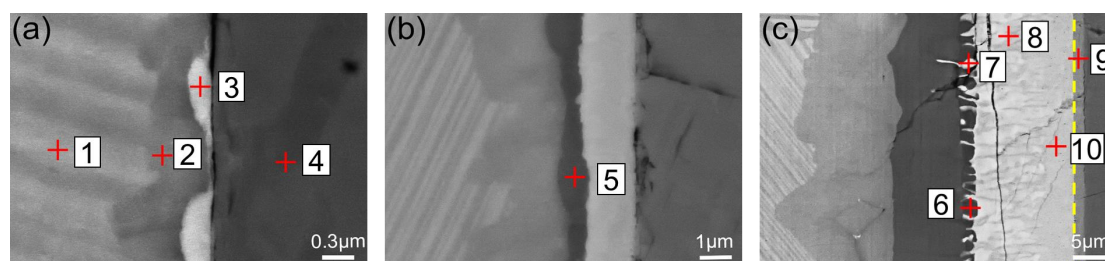


Fig. 1. Back-scattered electron images of the bonded TiAl/Ti3SiC2 joints for the bonding condition of (a) 900°C/15 min, (b) 950°C/1 h and (c) 1000°C/64 h.

Points	Elements Content (at. %)					Probable Phase	EBSD Results
	Ti	Al	Si	C	Nb		
1	55.8	37.9	-	2.2	4.1	α 2-Ti3Al	α 2-Ti3Al
2	50.9	44.0	0.2	1.8	3.1	γ -TiAl	γ -TiAl
3	53.3	6.9	31.5	6.4	1.9	Ti5Si3Cx	Ti5Si3Cx
4	52.9	-	15.2	31.9	-	Ti3SiC2	Ti3SiC2
5	33.1	61.1	0.2	2.7	2.9	TiAl2	TiAl2
6	24.8	62.3	6.6	2.3	3.9	Ti(Al, Si)3 or TiAl2	Ti(Al, Si)3
7	53.4	8.9	33.2	2.2	2.3	Ti5Si3Cx or Ti5Si4	Ti5Si3Cx
8	52.3	0.6	41.2	2.5	3.4	Ti5Si3Cx or Ti5Si4	Ti5Si4
9	54.5	1.9	33.7	9.6	0.3	Ti5Si3Cx or Ti5Si4	Ti5Si3Cx
10	53.0	1.8	35.5	6.4	3.3	Ti5Si3Cx or Ti5Si4	Ti5Si3Cx

Table 1. Elements quantitative analysis results of the points in Fig. 1 determined by EMPA.

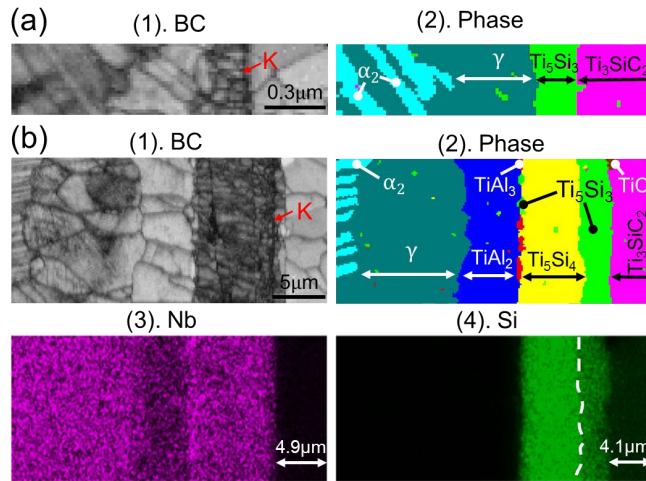


Fig. 2. Electron backscattered diffraction (EBSD) for the TiAl/Ti₃SiC₂ joints bonded at 900°C/15 min for (a) and 950°C/64 h for (b). (1) Bond contrast, (2) color-coded phase maps, and corresponding EDS elemental maps of (3) Nb, (4) Si. K is the mark for Kirkendall planes.

The cross sectional views of joints after etching are shown in Fig. 3 for the evolution of the interfacial microstructure analysis. The morphology and build-ups of the interfacial compounds were significantly influenced by the holding time and the bonding temperature. As Fig. 3(a) shows, the build-ups of interfacial phase in the joint bonded at 900°C/15 min was $\gamma+\alpha_2/\gamma/\text{Ti}_5\text{Si}_3/\text{Ti}_3\text{SiC}_2$. The build-up in the joint bonded at 900°C/0.5 h and 900°C/1 h were $\gamma+\alpha_2/\gamma/\text{Ti}_5\text{Si}_4/\text{Ti}_5\text{Si}_3/\text{Ti}_3\text{SiC}_2$ as shown in Fig. 3(b) and (c). When bonded at 950°C/15 min or 950°C/1 h, the interfaces consisted of $\gamma+\alpha_2/\gamma/\text{TiAl}_2/\text{Ti}_5\text{Si}_4/\text{Ti}_3\text{SiC}_2$ as shown in Fig. 3(d), (e). The interface bonded at 1000°C/64 h consisted of $\gamma+\alpha_2/\gamma/\text{TiAl}_2/\text{TiAl}_3+\text{Ti}_5\text{Si}_3/\text{Ti}_5\text{Si}_4/\text{Ti}_5\text{Si}_3/\text{Ti}_3\text{SiC}_2$, as shown in Fig. 3(f). A sequential phase growth, rather than a simultaneous phase growth, was found in the diffusion bonded TiAl/Ti₃SiC₂ joints. A similar result was reported in L. Hu's research [29]. The interfacial phases were formed in sequential order of $\text{Ti}_5\text{Si}_3 \rightarrow \text{Ti}_5\text{Si}_4 \rightarrow \text{TiAl}_2 \rightarrow \text{TiAl}_3$. The build-up of the interfacial compounds changed with the elongation of the duration, which was described as: $\gamma+\alpha_2/\text{Ti}_3\text{SiC}_2 \rightarrow \gamma+\alpha_2/\gamma/\text{Ti}_5\text{Si}_3/\text{Ti}_3\text{SiC}_2 \rightarrow \gamma+\alpha_2/\gamma/\text{Ti}_5\text{Si}_4/\text{Ti}_5\text{Si}_3/\text{Ti}_3\text{SiC}_2 \rightarrow \gamma+\alpha_2/\gamma/\text{TiAl}_2/\text{Ti}_5\text{Si}_4/\text{Ti}_5\text{Si}_3/\text{Ti}_3\text{SiC}_2 \rightarrow \gamma+\alpha_2/\gamma/\text{TiAl}_2/\text{TiAl}_3+\text{Ti}_5\text{Si}_3/\text{Ti}_5\text{Si}_4/\text{Ti}_5\text{Si}_3/\text{Ti}_3\text{SiC}_2$.

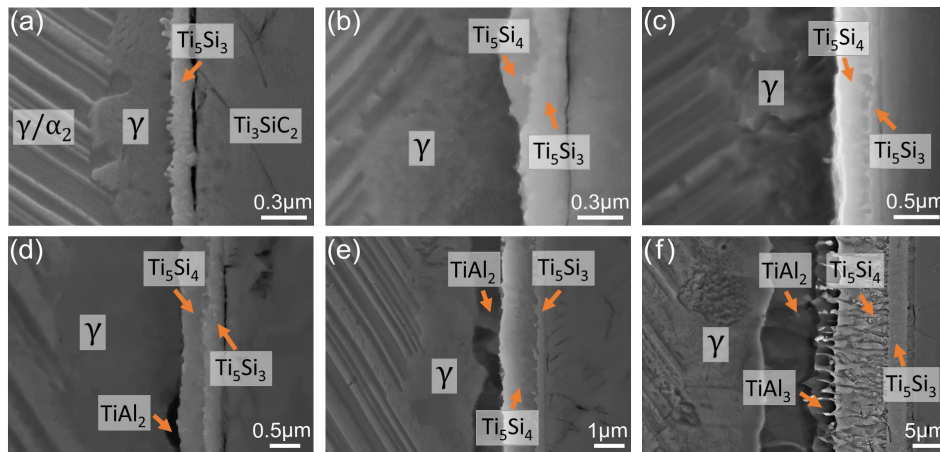


Fig. 3. Secondary electron images of the joints after etching under the bonding conditions of (a) 900°C/15 min, (b) 900°C/0.5 h, (c) 900°C/1 h, (d) 950°C/15 min, (e) 950°C/1 h, and (f) 1000°C/64 h.

The interfacial microstructure evolution and elements diffusion behaviors of the diffusion bonded TiAl/Ti₃SiC₂ joints are illustrated in Fig. 4. The Ti₅Si₃ and the γ -TiAl were the first two new layers

formed at the initial period of the diffusion bonding. The formation of Ti_5Si_3 was a result of the reaction of the out-diffusion Si atoms with the Ti atoms in TiAl base alloy as shown in Eq. (1). The Si atoms from the Ti_3SiC_2 diffusing into the TiAl base alloy was the main process. This demonstrated that the Si element was the fastest-diffusing specie in the Ti_3SiC_2 . The Si was the most weakly bonded element in the Ti_3SiC_2 [23, 24] and its vacancy formation energy was the smallest [25, 26]. The Ti_3SiC_2 was decomposed by the de-intercalation of Si, and which led to forming the non-stoichiometric $Ti_3Si_{1-x}C_2$ as per Eq. (2). The de-intercalated Si atoms diffused into the TiAl base alloy and reacted with the Ti element in the TiAl base alloy to form the Ti_5Si_3 layer, leaving the Al atoms to react with Ti_3Al and form the γ -TiAl layer as shown in Eq. (3). This finding agreed with the previous results showing that the out-diffusion of the “A” element into the other side was the main process during diffusion bonding [15, 17, 18].



There was a Kirkendall plane in the Ti_5Si_3 layer near the Ti_5Si_3/Ti_3SiC_2 boundary as illustrated in the Fig. 2(a) or (b). The diffusion flux of Si atoms from right to left was greater than the Ti atoms' in the opposite direction across the Kirkendall plane in Ti_5Si_3 layer. This meant the diffusion rate of the Si element was higher than the Ti element's in Ti_5Si_3 , which was similar to reported results in Ref. [29]. So, the Si was the fastest-diffusion element in the Ti_3SiC_2 and was the main diffusion element in the Ti_5Si_3 . These caused the diffusion of Si from the Ti_3SiC_2 to the TiAl base alloy to be the primary controlling process during the diffusion bonding, as shown in Fig. 4(a) and (b).

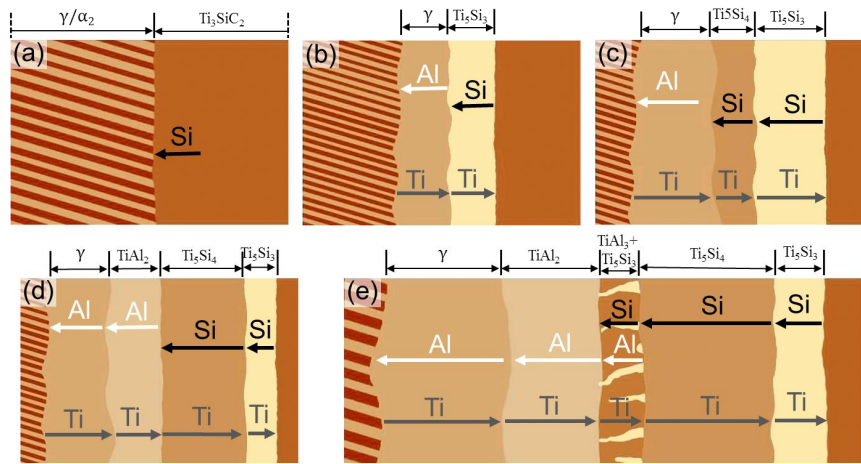


Fig. 4. Schematic representation of the interfacial microstructure evolution of the diffusion bonding TiAl/Ti₃SiC₂ joints.

As seen Fig. 1(a), the Ti_5Si_3 was the first new formation phase. Despite, the Ti_5Si_4 has a lower formation energy than the Ti_5Si_3 [30]. The Ti_5Si_3 obtained equilibrium interfaces (the equilibrium interface meant that the phase at both sides of the phase boundary were in thermodynamic equilibrium, and the phase boundary could exist in the equilibrium microstructure) both with the Ti_3SiC_2 and the γ -TiAl from the analysis of the phase graph in Fig. 5. This meant that the formation of Ti_5Si_3 may be controlled by the interfacial energy and the local equilibrium.

As the holding time increased, the de-intercalated Si atoms from the Ti_3SiC_2 substrate diffused across the Ti_5Si_3 layer and reacted with the Ti atoms diffusing from the γ -TiAl layer. The diffusion flux of Si atoms could be more than the flux consumed by the reaction with Ti, so the Si atoms accumulated at the γ -TiAl/ Ti_5Si_3 phase boundary and caused the formation of the Ti_5Si_4 . The Ti_5Si_3 tended to transform into the Ti_5Si_4 , because the Ti_5Si_4 had a lower formation energy [30]. This may be another cause of the Ti_5Si_4 formation.

The out-diffusing of the Si atoms reacting with the Ti atoms and expelling the Al atoms caused the expelled Al atoms to diffuse from the γ /Ti₅Si₃ phase boundary to the TiAl substrate and the Ti atoms diffused in the opposite direction, as shown in Fig. 4(b). The Al element had a poorer diffusivity than the Ti element in the γ -TiAl at the recorded temperature [38], causing the accumulation of Al atoms at the interface. With the increased accumulation of the Al at the γ -TiAl/Ti₅Si₄ interface, the TiAl₂ nucleated when the Al concentration reached the solubility limitation of the γ -TiAl, as shown in Fig. 4(d). Fig. 2(b) shows that the large TiAl₂ grains covered the thickness from the Ti₅Si₄/TiAl₂ boundary to the TiAl₂/ γ -TiAl boundary.

The TiAl₂/Ti₅Si₄ phase boundary was not an equilibrium interface from the phase graph in Fig. 5. A dual TiAl₃ and Ti₅Si₃ phase layer formed at the interface of the TiAl₂ and the Ti₅Si₃ as shown in Fig. 4(e). The formation of TiAl₃ might be a result of the further accumulation of the Al atoms at the interface between TiAl₂ and Ti₅Si₄. The Si atoms diffused from the Ti₅Si₄ into TiAl₃ and caused the formation of the Ti₅Si₃. The formation of the dual phase layer could reduce the energy of the TiAl₂/Ti₅Si₄ interface, because the TiAl₃ and Ti₅Si₃ dual phase layer could obtain equilibrium interfaces both with TiAl₂ and Ti₅Si₄ as shown in Fig. 5.

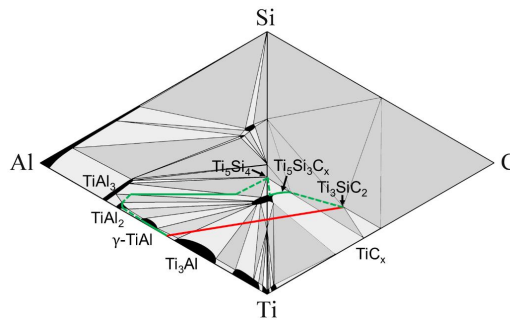


Fig. 5: The ternary phase graphs of the Ti-Si-Al and the Ti-Si-C according data from previous research [30, 32, 33].

The final structure of the TiAl/Ti₃SiC₂ diffusion bonding joint was $\gamma + \alpha_2 / \gamma / \text{TiAl}_2 / \text{Ti}_5\text{Si}_3 + \text{TiAl}_3 / \text{Ti}_5\text{Si}_4 / \text{Ti}_5\text{Si}_3 / \text{Ti}_3\text{SiC}_2$. The diffusion path (green line) did not intersect with the line between the two substrates (red line) as illustrated in Fig. 5, which did not satisfy the rule proposed by Van Loo [34] stating that the diffusion path must cross the straight line between the end-members of the reaction couple at least once for mass balance. This meant that the reactions at the joint were not mass balanced. These could be explained that the Si acted as a long-term diffusion element in the Ti₃SiC₂ and the Ti₃SiC₂ could transform into the Ti₃Si_{1-x}C₂ by de-interaction of Si. The diffusion couple was considered a couple of the Si and TiAl base alloys, which satisfied the mass balance.

3.2 Growth kinetics of the interfacial compound layers

The thicknesses of each reaction layer, Ti₅Si₃, Ti₅Si₄, TiAl₂, and TiAl₃ + Ti₅Si₃ dual phase layers, were measured at each bonding condition according the BSE and the SE image. The thicknesses and the standard deviations were calculated from an average of at least 3 measurements for each bonding condition. Fig. 6 shows the plot of each layer thickness versus the square root of the bonding time and temperature. As the holding time increased at each temperature, the thickness of each layer of the diffusion bonding TiAl/Ti₃SiC₂ joints increased. The higher growth rate was obtained at a higher bonding temperature. Good linear relationships were observed, as shown in Fig. 6, indicating that the growth of each interfacial layer thickness followed the parabolic kinetic law, i.e. $x^2 = 2K_p \cdot t$, where x is the thickness of each interfacial layer, K_p is the parabolic rate constant, and t is the holding time. It demonstrated the growth of each interlayer was controlled by the bulk diffusion [35]. The holding time before the formation of the TiAl₂ or TiAl₃, termed the incubation time, shortened when the temperature rose. The incubation time of TiAl₃ at 900°C was about 64 h, but 4 h at 1000°C. Parabolic rate constants (K_p) of each layer was obtained for each bonding temperature, see the slopes

of the curves shown in Fig. 7(a), 7(b), and 7(c). The thicknesses of TiAl₃ was too small to be measured accurately, so the parabolic rate constant of the TiAl₃ was not calculated.

The parabolic rate constants were further exploited to determine the activation energies for each growth layer according to the Arrhenius equation $K_p = A \cdot \exp(-Q/RT)$, where A is the pre-exponent factor, Q is the bonding activation energy, R is the universal gas constant, and T is the absolute temperature. The Ln(K_p) was plotted as a function of the bonding temperature in the temperature range between 900-1000°C. A good linear relationship was found between the Ln(K_p) and the inverse of temperature, the result is shown in Fig. 6(d). The bonding activation energy of the TiAl/Ti₃SiC₂ joints was 213 kJ/mol from the slope of the Arrhenius plot using a linear regression model, which was higher than the activation energy values reported in previous literature: 156 kJ/mol for TC4/Ti₃SiC₂ [9], 170 kJ/mol for Ti₃SiC₂/Zr-4 [36], and 120 kJ/mol for NiTi/Ti₃SiC₂ [11] diffusion couples. The higher the activation energy may be due to the poorer diffusivity of the Si in TiAl base alloy than in the TC4, Zr-4 or NiTi. The growth activation energy of the Ti₅Si₃, the Ti₅Si₄, and the TiAl₂ were deviated to be 378 kJ/mol, 199 kJ/mol, and 214 kJ/mol.

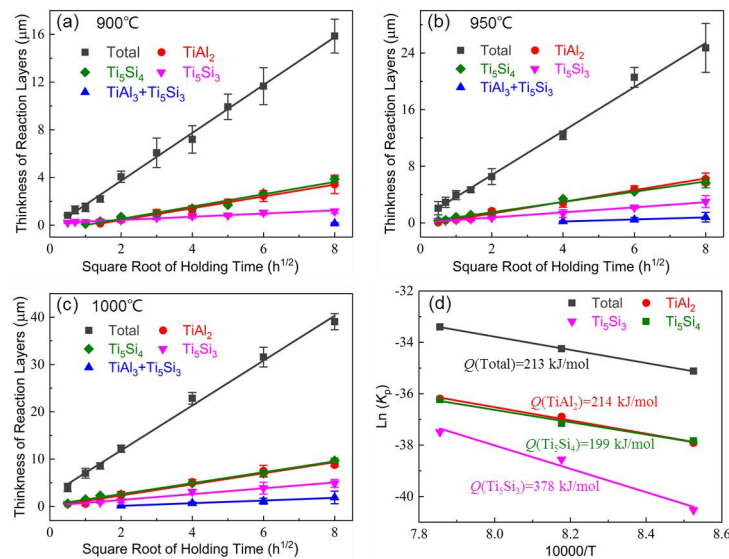


Fig. 6. The evolution of the interfacial reaction layer thickness with the square root of holding time at temperature of (a) 900°C, (b) 950°C, and (c) 1000°C. (d) The Arrhenius plot of the parabolic rate constant versus the reciprocal of the absolute bonding temperature ranged between 900-1000°C.

3.3 Shear strength and Fracture morphologies

The joining properties of the diffusion bonded TiAl/Ti₃SiC₂ joints were evaluated via a shear strength test, see Fig. 7. The shear strength test results showed that the shear strength first increased, then decreased as the holding time is increased at the each treat temperature. The maximum value of the shear strength at each temperature decreased as the bonding temperature increased. The failure of the joint first occurred at the initial TiAl/Ti₃SiC₂ interface, then mainly occurred at the Ti₃SiC₂ side, and then occurred in the Ti₅Si₃ and Ti₅Si₄ reaction layers with the increment of the holding times.

The low shear strength of joints bonded for a short holding time at each bonding temperature was caused by the existence of pores at the interface and the un-metallurgical bonding interface as shown in Fig. 1(a), Fig. 3(a) and (d). The different coefficient of the thermal expansion (CTE) between the Ti₃SiC₂ and the TiAl base alloy [31, 39] caused the residual stress to generate at the interfacial region during the cooling stage, which degraded the joining properties. A relatively higher bonding temperature led to a larger residual stress value, which resulted in a more severe crack tendency. So, the maximum value of bonding joints decreased as the temperature increased.

So, the build-ups and thickness of the interfacial layers have a great influence on the strength of joints. The pores, un-metallurgical bonding interface, and thick Ti_xSi_y layers were responsible for the poor bond strength. The shear strength of the joint will great be deteriorated when thickness of the

Ti₅Si₄ layers is greater than 2.5 μm. The highest bonding strength was about 53 MPa at 900°C for 9 h with a $\gamma+\alpha_2/\gamma/\text{TiAl}_2/\text{Ti}_5\text{Si}_4/\text{Ti}_5\text{Si}_3/\text{Ti}_3\text{SiC}_2$ interfacial microstructure. At this bonding condition, the thickness of the Ti₅Si₄ and Ti₅Si₃ layers was about 1.4 μm, and the total thickness of all the interfacial layers was about 6 μm. While, the values of the shear strength in Ref. [12] are no more than 20 MPa. This could be because the high bonding temperature led to the formation of high residual stress and propagation of the micro cracks in the thick Ti₅Si₄ and Ti₅Si₃ layers.

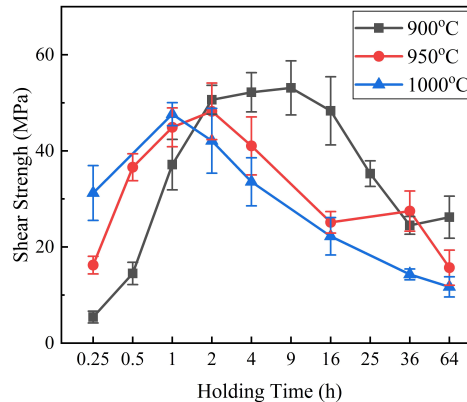


Fig. 7. Shear strength of the TiAl/Ti₃SiC₂ diffusion bonding joints under various holding times at 900°C, 950°C and 1000°C.

4. Conclusions

The TiAl base alloy and the Ti₃SiC₂ ceramic were successfully joined using the direct diffusion bonding. The evolution of the interfacial microstructure, the elements diffusion behaviors, the growth kinetics, and the mechanical properties of the joints were investigated. Conclusions are summarized as follows.

(1) The structures of the interfacial microstructure changed from $\gamma+\alpha_2/\gamma/\text{Ti}_5\text{Si}_3/\text{Ti}_3\text{SiC}_2$, to $\gamma+\alpha_2/\gamma/\text{TiAl}_2/\text{Ti}_5\text{Si}_3/\text{Ti}_3\text{SiC}_2$, to $\gamma+\alpha_2/\gamma/\text{TiAl}_2/\text{Ti}_5\text{Si}_4/\text{Ti}_5\text{Si}_3/\text{Ti}_3\text{SiC}_2$, and to $\gamma+\alpha_2/\gamma/\text{TiAl}_2/\text{TiAl}_3+\text{Ti}_5\text{Si}_3/\text{Ti}_5\text{Si}_4/\text{Ti}_5\text{Si}_3/\text{Ti}_3\text{SiC}_2$ as the time or bonding temperature increased. The formation sequence of the interfacial compounds was as follows: Ti₅Si₃ → Ti₅Si₄ → TiAl₂ → TiAl₃. The de-intercalation Si atoms from the Ti₃SiC₂ diffused into the TiAl base alloy and reacted with the Ti elements as the primary process during the diffusion bonding.

(2) The growth of each interfacial layers was controlled by the bulk diffusion. Their growth kinetics obeyed the parabolic law. The bonding activation energy of the joint was 213 kJ/mol. The growth activation energy of Ti₅Si₃, Ti₅Si₄, and TiAl₂ deviated to be 378 kJ/mol, 199 kJ/mol, and 214 kJ/mol.

(3) The highest shear strength of the joint was about 53 MPa bonded at 900°C for 9 h with a $\gamma+\alpha_2/\gamma/\text{TiAl}_2/\text{Ti}_5\text{Si}_4/\text{Ti}_5\text{Si}_3/\text{Ti}_3\text{SiC}_2$ interfacial microstructure. The thick Ti₅Si₄ and Ti₅Si₃ layers deteriorated the property of the joints.

ACKNOWLEDGEMENTS

This work was supported by the National Natural Science Foundation of China [grant numbers U1908229, 51675078, 51175059].

REFERENCES

- [1] Y.-W. Kim, Ordered intermetallic alloys, part III: Gamma titanium aluminides, JOM 46(7) (1994) 30-39. <https://doi.org/10.1007/bf03220745>
- [2] M. Yamaguchi, H. Inui, K. Ito, High-temperature structural intermetallics, Acta Mater. 48(1) (2000) 307-322. [https://doi.org/10.1016/S1359-6454\(99\)00301-8](https://doi.org/10.1016/S1359-6454(99)00301-8)

- [3] D.M. Dimiduk, Gamma titanium aluminide alloys—an assessment within the competition of aerospace structural materials, *Mater. Sci. Eng. A* 263(2) (1999) 281-288. [https://doi.org/10.1016/S0921-5093\(98\)01158-7](https://doi.org/10.1016/S0921-5093(98)01158-7)
- [4] T. Tetsui, Application of TiAl in a Turbocharger for Passenger Vehicles, *Adv. Eng. Mater.* 3(5) (2001) 307-310. [https://doi.org/10.1002/1527-2648\(200105\)3:5<307::AID-ADEM307>3.0.CO;2-3](https://doi.org/10.1002/1527-2648(200105)3:5<307::AID-ADEM307>3.0.CO;2-3)
- [5] P. Janschek, Wrought TiAl blades, *Mater. Today-Proceedings 2(Supplement 1)* (2015) S92-S97. <https://doi.org/10.1016/j.matpr.2015.05.024>
- [6] O.M. Akselsen, Diffusion Bonding of Ceramics, *J. Mater. Sci.* 27(3) (1992) 569-579. <https://doi.org/10.1007/Bf02403862>
- [7] Y. Nakao, K. Shinozaki, M. Hamada, Diffusion Bonding of Intermetallic Compound TiAl, *ISIJ Int.* 31(10) (1991) 1260-1266. <https://doi.org/10.2355/isijinternational.31.1260>
- [8] S. Basu, M.F. Ozaydin, A. Kothalkar, I. Karaman, M. Radovic, Phase and morphology evolution in high-temperature Ti₃SiC₂-NiTi diffusion-bonded joints, *Scr. Mater.* 65(3) (2011) 237-240. <https://doi.org/10.1016/j.scriptamat.2011.04.015>
- [9] N.F. Gao, Y. Miyamoto, Joining of Ti₃SiC₂ with Ti-6Al-4V Alloy, *J. Mater. Res.* 17(01) (2011) 52-59. <https://doi.org/10.1557/jmr.2002.0010>
- [10] J. Cao, J.K. Liu, X.G. Song, X.T. Lin, J.C. Feng, Diffusion bonding of TiAl intermetallic and Ti₃AlC₂ ceramic: Interfacial microstructure and joining properties, *Mater. Des.* 56 (2014) 115-121. <https://doi.org/10.1016/j.matdes.2013.10.074>
- [11] A. Kothalkar, A. Cerit, G. Proust, S. Basu, M. Radovic, I. Karaman, Interfacial study of NiTi-Ti₃SiC₂ solid state diffusion bonded joints, *Mater. Sci. Eng. A* 622 (2015) 168-177. <https://doi.org/10.1016/j.msea.2014.10.033>
- [12] J.K. Liu, J. Cao, X.G. Song, Y.F. Wang, J.C. Feng, Evaluation on diffusion bonded joints of TiAl alloy to Ti₃SiC₂ ceramic with and without Ni interlayer: Interfacial microstructure and mechanical properties, *Mater. Des.* 57 (2014) 592-597. <https://doi.org/10.1016/j.matdes.2014.01.029>
- [13] L.F. Hu, A. Kothalkar, G. Proust, I. Karaman, M. Radovic, Fabrication and characterization of NiTi/Ti₃SiC₂ and NiTi/Ti₂AlC composites, *J. Alloys Compd.* 610 (2014) 635-644. <https://doi.org/10.1016/j.jallcom.2014.04.224>
- [14] Z.S. Xu, B. Xue, X.L. Shi, Q.X. Zhang, W.Z. Zhai, J. Yao, Y.F. Wang, Sliding Speed and Load Dependence of Tribological Properties of Ti₃SiC₂/TiAl Composite, *Tribol. Trans.* 58(1) (2015) 87-96. <https://doi.org/10.1080/10402004.2014.951748>
- [15] S. Wang, J. Cheng, S. Zhu, Z. Qiao, J. Yang, W. Liu, Microstructure evolution, mechanical and tribological properties of Ti₃(Al,Sn)C₂/Al₂O₃ composites, *J. Eur. Ceram. Soc.* 38(6) (2018) 2502-2510. <https://doi.org/10.1016/j.jeurceramsoc.2018.01.029>
- [16] V. Pasumarthi, Y. Chen, S.R. Bakshi, A. Agarwal, Reaction synthesis of Ti₃SiC₂ phase in plasma sprayed coating, *J. Alloys Compd.* 484(1-2) (2009) 113-117. <https://doi.org/10.1016/j.jallcom.2009.04.079>
- [17] F.F. Qi, Z. Wang, J.Y. Wu, H.G. Xu, J.J. Kou, L. Zhang, Improved mechanical properties of Al₂O₃ ceramic by in-situ generated Ti₃SiC₂ and TiC via hot pressing sintering, *Ceram. Int.* 43(14) (2017) 10691-10697. <https://doi.org/10.1016/j.ceramint.2017.04.165>
- [18] J. Zhang, W. Liu, Y. Jin, S. Wu, T. Hu, Y. Li, X. Xiao, Study of the interfacial reaction between Ti₃SiC₂ particles and Al matrix, *J. Alloys Compd.* 738 (2018) 1-9. <https://doi.org/https://doi.org/10.1016/j.jallcom.2017.12.123>
- [19] Z.F. Zhang, Z.M. Sun, H. Hashimoto, Rapid synthesis of ternary carbide Ti₃SiC₂ through pulse-discharge sintering technique from Ti/Si/TiC powders, *Metall. Mater. Trans. A* 33(11) (2002) 3321-3328. <https://doi.org/10.1007/s11661-002-0320-1>
- [20] V.A. Baheti, S. Kashyap, P. Kumar, K. Chattopadhyay, A. Paul, Bifurcation of the Kirkendall marker plane and the role of Ni and other impurities on the growth of Kirkendall voids in the Cu-Sn system, *Acta Mater.* 131 (2017) 260-270. <https://doi.org/10.1016/j.actamat.2017.03.068>
- [21] A. Paul, T. Laurila, V. Vuorinen, S.V. Divinski, Interdiffusion and the Kirkendall Effect in Binary Systems, in: A. Paul, T. Laurila, V. Vuorinen, S.V. Divinski (Eds.), *Thermodynamics, Diffusion and the Kirkendall Effect in Solids*, Springer International Publishing, Cham, 2014, pp. 239-298. https://doi.org/10.1007/978-3-319-07461-0_6

- [22] L.F. Hu, Y.Z. Xue, F.R. Shi, Intermetallic formation and mechanical properties of Ni-Ti diffusion couples, *Mater. Des.* 130 (2017) 175-182. <https://doi.org/10.1016/j.matdes.2017.05.055>
- [23] H.Z. Zhang, S.Q. Wang, First-principles study of Ti₃AC₂ (A=Si, Al) (001) surfaces, *Acta Mater.* 55(14) (2007) 4645-4655. <https://doi.org/10.1016/j.actamat.2007.04.033>
- [24] C.M. Fang, R. Ahuja, O. Eriksson, S. Li, U. Jansson, O. Wilhelmsson, L. Hultman, General trend of the mechanical properties of the ternary carbides M₃SiC₂ (M=transitionmetal), *Phys. Rev. B* 74(5) (2006). <https://doi.org/10.1103/PhysRevB.74.054106>
- [25] L.X. Jia, Y.X. Wang, X.D. Ou, L.Q. Shi, W. Ding, Decohesion of Ti₃SiC₂ induced by He impurities, *Mater. Lett.* 83 (2012) 23-26. <https://doi.org/10.1016/j.matlet.2012.05.093>
- [26] H.B. Zhang, J.M. Wang, J.Y. Wang, Y.C. Zhou, S.M. Peng, X.G. Long, Role of Nanolaminated Crystal Structure on the Radiation Damage Tolerance of Ti₃SiC₂: Theoretical Investigation of Native Point Defects, *J. Nanomater.* 2013 (2013) 1-5. <https://doi.org/10.1155/2013/831590>
- [27] J.Y. Wu, Y.C. Zhou, J.Y. Wang, W. Wang, C.K. Yan, Interfacial reaction between Cu and Ti₂SnC during processing of Cu-Ti₂SnC composite, *Zeitschrift Fur Metallkunde* 96(11) (2005) 1314-1320. <https://doi.org/10.3139/146.101181>
- [28] S. Wang, J. Cheng, S.Y. Zhu, J.Q. Ma, Z.H. Qiao, J. Yang, W.M. Liu, A novel route to prepare a Ti₃SnC₂/Al₂O₃ composite, *Scr. Mater.* 131 (2017) 80-83. <https://doi.org/10.1016/j.scriptamat.2017.01.013>
- [29] S. Roy, S. Prasad, S.V. Divinski, A. Paul, Diffusion pattern in MSi₂ and M₅Si₃ silicides in group VB (M=V, Nb, Ta) and VIB (M=Mo, W) refractory metal-silicon systems, *Philos. Mag.* 94(14) (2014) 1508-1528. <https://doi.org/10.1080/14786435.2014.888103>
- [30] Y. Li, Q.-F. Gu, Q. Luo, Y. Pang, S.-L. Chen, K.-C. Chou, X.-L. Wang, Q. Li, Thermodynamic investigation on phase formation in the Al-Si rich region of Al-Si-Ti system, *Mater. Des.* 102 (2016) 78-90. <https://doi.org/10.1016/j.matdes.2016.03.144>
- [31] C. Herzig, T. Przeorski, Y. Mishin, Self-diffusion in γ -TiAl: an experimental study and atomistic calculations, *Intermetallics* 7(3-4) (1999) 389-404. [https://doi.org/10.1016/s0966-9795\(98\)00117-4](https://doi.org/10.1016/s0966-9795(98)00117-4)
- [32] Y. Du, J.C. Schuster, H.J. Seifert, F. Aldinger, Experimental investigation and thermodynamic calculation of the titanium-silicon-carbon system, *J. Am. Ceram. Soc.* 83(1) (2000) 197-203. <https://doi.org/10.1111/j.1151-2916.2000.tb01170.x>
- [33] Z. Li, C.L. Liao, Y.X. Liu, X.M. Wang, Y. Wu, M.X. Zhao, Z.H. Long, F.C. Yin, 700 degrees C Isothermal Section of the Al-Ti-Si Ternary Phase Diagram, *J. Phase Equilibria Diffus.* 35(5) (2014) 564-574. <https://doi.org/10.1007/s11669-014-0325-7>
- [34] A.A. Kodentsov, G.F. Bastin, F.J.J. van Loo, The diffusion couple technique in phase diagram determination, *J. Alloys Compd.* 320(2) (2001) 207-217. [https://doi.org/10.1016/S0925-8388\(00\)01487-0](https://doi.org/10.1016/S0925-8388(00)01487-0)
- [35] U. Gösele, K.N. Tu, Growth kinetics of planar binary diffusion couples: "Thin - film case" versus "bulk cases", *J. Appl. Phys.* 53(4) (1982) 3252-3260. <https://doi.org/10.1063/1.331028>
- [36] D.J. Tallman, J. Yang, L. Pan, B. Anasori, M.W. Barsoum, Reactivity of Zircaloy-4 with Ti₃SiC₂ and Ti₂AlC in the 1100–1300°C temperature range, *J. Nucl. Mater.* 460 (2015) 122-129. <https://doi.org/10.1016/j.jnucmat.2015.02.006>
- [37] K. Kishida, M. Fujiwara, H. Adachi, K. Tanaka, H. Inui, Plastic deformation of single crystals of Ti₅Si₃ with the hexagonal D88 structure, *Acta Mater.* 58(3) (2010) 846-857. <https://doi.org/10.1016/j.actamat.2009.09.062>
- [38] T.H. Scabarozzi, S. Amini, O. Leaffer, A. Ganguly, S. Gupta, W. Tambussi, S. Clipper, J.E. Spanier, M.W. Barsoum, J.D. Hettinger, S.E. Lofland, Thermal expansion of select Mn+1AX_n (M=earlytransitionmetal, A=A group element, X=C or N) phases measured by high temperature x-ray diffraction and dilatometry, *J. Appl. Phys.* 105(1) (2009) 013543. <https://doi.org/10.1063/1.3021465>
- [39] Y. He, R.B. Schwarz, T. Darling, M. Hundley, S.H. Whang, Z.M. Wang, Elastic constants and thermal expansion of single crystal gamma-TiAl from 300 to 750 K, *Mater. Sci. Eng. A* 240 (1997) 157-163. [https://doi.org/10.1016/S0921-5093\(97\)00575-3](https://doi.org/10.1016/S0921-5093(97)00575-3)